Insights into the Suzuki-Miyaura Reaction Catalyzed by Pd -Carbene Complexes: Are Palladium-Tetracarbene Species the Key Actives Species?

Jonathan de Tovar, F. Rataboul, Laurent Djakovitch

▶ **To cite this version:**

Jonathan de Tovar, F. Rataboul, Laurent Djakovitch. Insights into the Suzuki-Miyaura Reaction Catalyzed by Pd -Carbene Complexes: Are Palladium-Tetracarbene Species the Key Actives Species?. ChemCatChem, 2020, 12 (22), pp.5797-5808. 10.1002/cctc.202001253 . hal-03367104

HAL Id: hal-03367104
https://hal.science/hal-03367104

Submitted on 6 Oct 2021

HAL is a multi-disciplinary open access archive for the deposit and dissemination of scientific research documents, whether they are published or not. The documents may come from teaching and research institutions in France or abroad, or from public or private research centers.

L'archive ouverte pluridisciplinaire **HAL**, est destinée au dépôt et à la diffusion de documents scientifiques de niveau recherche, publiés ou non, émanant des établissements d'enseignement et de recherche français ou étrangers, des laboratoires publics ou privés.

New Insights into the Suzuki-Miyaura Reaction Catalyzed by Pd – Carbene Complexes: Are Palladium-Tetracarbene Species the Key Actives Species?

Jonathan De Tovar,*,† Franck Rataboul,† Laurent Djakovitch*,†

† Université de Lyon, Université Claude Bernard Lyon 1, CNRS, IRCELYON, F-69626, Villeurbanne, France

ABSTRACT: The assumption that the real active species involved in the Suzuki-Miyaura reaction are homogeneous, heterogeneous or both is often proposed. However a lack in the characterization of true catalytic entities and their monitoring makes assumptions somewhat elusive. Here, three families of palladium(II) complexes bearing bisNHC, bispyridyl and bisphosphine ligands were synthetized in order to get new insights into the formation of active species in the Suzuki-Miyaura reaction. Their comparative catalytic study reveals that the nature of the ligands as well as their spacer lengths are pivotal parameters governing the performance. All complexes evolve to Pd NPs under reaction conditions, and an orthogonal behavior is observed for two bisNHC complexes that form homoleptic tetracarbene species. Notably, these species are presumably involved in a new catalytic modus operandi. This ligand-controlled reactivity and the formation of tetracarbene species open new routes towards the design of novel cross-coupling catalysts via the mastering of highly-active catalytic species.

■ INTRODUCTION

Palladium-catalyzed cross-coupling reactions are of paramount importance from an industrial point of view.[1] In particular, the Suzuki-Miyaura reaction allows to easily form biaryls intermediates useful in organic synthesis.[2] This reaction is catalyzed mainly using palladium species giving generally high activities.

Well-defined palladium molecular complexes and nanoparticles (NPs) have been tested in this reaction.[3] A controversy concerning the exact nature of the real catalytic system (the catalytic active species) exists under turnover conditions.[4-6] For instance, very active catalytic species such as NPs evolved from molecular complexes are quite often postulated but their exact nature is elusive.[7,8]

In molecular complexes, the structure and electronic properties of the ligand coordinated to the metal core are pivotal factors influencing not only the activity, selectivity and stability of the catalysts[9,10] but also their evolution to the real catalysts or depletion to bulk palladium.[11] Due to the good stability and coordination capability, pyridyls serve as *N*-ligands for some transition metal-catalyzed reactions, especially redox reactions.[12,13] In addition, as an alternative to phosphines, the remarkably strong σ–binding and π-backdonation characters, steric tunability and high stability under oxidative conditions of *N*-heterocyclic carbene (NHC) ligands provide them the ability to stabilize highly unusual and hitherto elusive reactive species such as metal nanoparticles.[14,15] Chelating ligands are believed to provide additional catalyst stability under turnover conditions, and several studies describe the preparation and applications of biscarbene-bridged palladium(II) complexes in such C-C coupling reactions.[16-23] For example, Jothibasu and Huynh prepared a series of palladium(II) complexes bearing *cis*-chelating *homodicarbene* ligands varying bridges and N-heterocyclic backbones. Results for the Mizoroki-Heck reaction revealed superior activities for methylene- and propylene-bridged dibenzimidazol-2-ylidenes ligands.[21]

However, although some general trends have been introduced for the Mizoroki-Heck reaction, a deep study based on the spacer-length unit and ligand nature has not been, to the best of our knowledge, reported for the Suzuki-Miyaura reaction. Additionally, despite the extensive catalyst evolution and *in situ* transformation revealed for nanoparticles in catalysis, Pd-NHC systems dynamics remain still unraveled for such a C-C coupling reaction.

In this work we studied the evolution of palladium complexes of the type $PdX_2(L\cap L)$, in which L∩L is a chelating bis(benzimidazol-2-ylidene) ligand, in the Suzuki-

Miyaura reaction to identify the nature of the active species generated from such complexes. For that we particularly evaluated (a) the effect of the spacer-length (∩), (b) the influence of coordination of the ligand, (c) the nature of the substrate and (d) the effect of the temperature. For this comparison we also studied the influence of bispyridyl and bisphosphine ligands. Indeed, one can speculate that Pd species in the reaction medium can be controlled by the nature of the selected bidentate ligands from which it is expected an easier decoordination for bisphosphine ligands relative to bispyridyl and biscarbene ligands under same reaction conditions.

■ RESULTS AND DISCUSSION

Synthesis and Characterization of Bidentate-Ligands and Complexes. The synthetic strategy followed for the preparation of ligands is outlined in Scheme 1. It is based on alkylation of benzimidazole with bromopropane followed by a subsequent substitution reaction with different dihaloalkanes. Ligands **3a-c** were fully characterized by NMR (1D and 2D, see Experimental section and Figures S1-S3). ^{1}H NMR spectra indicate a C_2 symmetry in solution for the three ligands in which not only the two alkylated benzimidazolium moieties are equivalent but also the bridge protons. All ligands have also been characterized by HR-ESI-MS (Figures S4-S6) and IR spectroscopy (Figures S7-S9).

Palladium(II) molecular complexes of **3a-c** have been synthesized in order to evaluate the coordination properties of these ligands as well as their influence when resulting Pd complexes were engaged in the Suzuki-Miyaura reactions. **C1a-c** were prepared following the temperature program of Ahrens *et al.*[24] directly reacting palladium(II) acetate with the different bisbenzimidazolium salts in hot DMSO (Scheme 1).

Scheme 1. Synthetic Pathway for 3a-c Ligands and C1a-c Complexes

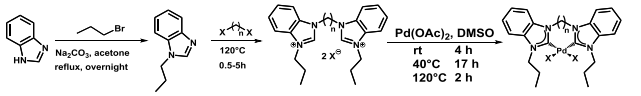

All Pd(II) complexes have been obtained as air- and moisture-stable solids. ^{1}H NMR spectra of **C1a-c** complexes show that the downfield signals (9-11 ppm) of pre-carbene protons for the different bisbenzimidazolium salts are no longer present (Figures S10-S12), thus confirming the deprotonation of the benzimidazolium moiety and formation of biscarbene complexes. Additionally, all methylene protons of the bridges become diastereotopic due to ligand coordination and retention of the bend-boat conformation in these complexes.[17] The observed broadening of these resonances has been attributed to the fluxionality of the seven- or eight-membered chelate rings.[21] Interestingly, because of the strong interaction with iodo or bromo groups, the methylene protons of propyl chains became also diastereotopic, being shifted downfield (4-5 ppm). Scherg *et al.* prepared similar complexes and determined high coalescence temperatures at which the inequivalent protons become isotopic.[17] The formation of the **C1a-c** mononuclear complexes is supported by base peaks in their ESI high-resolution mass spectra at m/z = 565.0075 and 593.0384 for the molecular cations $[M\text{-}I]^+$ (**C1a** and **C1c**, respectively, Figures S13 and S15), and 533.0358 for the molecular cation $[M\text{-}Br]^+$ (**C1b**, Figure S14). Finally, the formation of the complexes has been attested by IR spectroscopy (Figures S16-S18).

Single crystals suitable for X-ray diffraction analyses for **C1a-c** complexes were obtained by slow evaporation of saturated DMF solutions for **C1a** and **C1c** and a saturated DMSO solution for **C1b**. Molecular plots of **C1a-c** are shown in Figure 1, and selected crystallographic data, bond distances and angles are collected in Tables S1 and S2. The whole **C1a-c** complex family crystallized in a monoclinic crystal system. All complexes show a *cis*-geometry around a slightly distorted square-planar palladium center, with the two halide twisted out of the PdC_2 plane by 3.5(9)-11.2(1). The Pd-C coordination bond lengths in the three complexes are rather similar and in agreement with those in similar complexes reported before.[21] The C1-Pd-C21 bite angle changes slightly upon lengthening of the bridging moiety, from 82.4(3)° for **C1a** to 86.1(3)° and 85.1(3)° for **C1b** and **C1c**, respectively. Compared to the chelating bisdiphenylphosphino alkanes, where every additional methylene moiety in the bridging chain leads to an increase in bite angle of 4.8-13.1°, this is a relatively small difference.[26] This smaller effect in the bite angle is due to the angle at which the benzimidazole rings are twisted relative to the coordination plane (Table S1),[26] being quasi perpendicular for longer bridging moieties.[24] This indicates a greater steric demand by the ligands that is supported by the distance of the propyl groups, which shields the metal from the lower side of the complex.[26] Accordingly, the distance became shorter with growing bridge length (**C1a**: 3.584, 3.606 Å, **C1b**: 3.381, 3.546 Å; **C1c**: 3.477, 3.493 Å). Noticeably, this twist provokes asymmetric crystallization of the complexes. The most important feature of these structures are the interactions between protons from bridge or propyl chain and palladium(II) core (C-H···Pd, Figures S19-S21). For **C1b**, the bond lengths and angles indicate strong agostic interactions since the distance between the hydrogen atoms and the palladium(II) core are shorter than the sum of their van der Waals radii. However, for **C1c** complex, the bond lengths and angles indicate that these interactions are anagostic.[29] Interestingly for **C1a**, although the distance of Pd and the H11a bridge proton is larger than the sum of their van der Waals radii, the angle

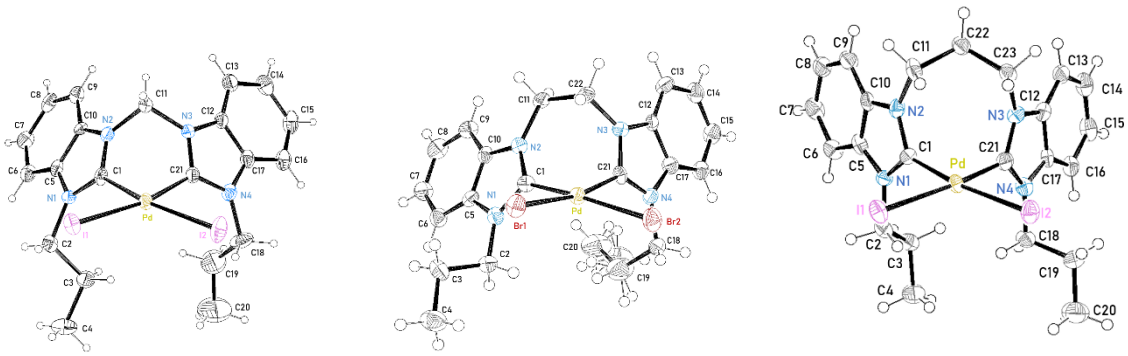

C1a **C1b** **C1c**

Figure 1. Displacement ellipsoid plots of **C1a-c** complexes at the 50% probability level. Solvent molecules are omitted for clarity.

of 87.03° and the fixed boat conformation indicate a pseudo-agostic interaction. Nevertheless, the presence of all these weak interactions supports the downfield shift of the methylene moieties in the ^{1}H NMR spectra (*vide supra*). The bridges and propyl chains show staggered conformations along their bonds, as expected. Details of the structure determinations are given in the Experimental section and Supplementary material (Appendix A).

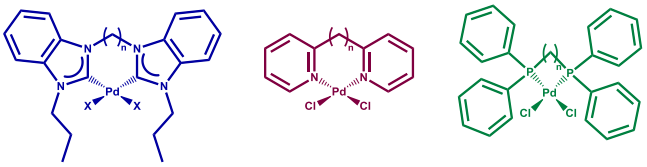

Figure 2. Catalysts prepared and used in this work.

As indicated above, with the aim to evaluate the nature of the ligand, bispyridyl-based **C2a-c** and bisphosphine-based **C3a-c** complexes (Figure 2) have been prepared for comparison purposes following reported procedures.[25,29,30]

Catalytic Performance in the Suzuki-Miyaura Reaction. The different prepared palladium(II) complexes have been evaluated as catalysts for the model reaction depicted in Scheme 2 (Tables 3 and 4). We aimed at performing the reactions under mild conditions and short times using low catalyst loading.

Scheme 2. Suzuki-Miyaura Reaction Studied in this Work

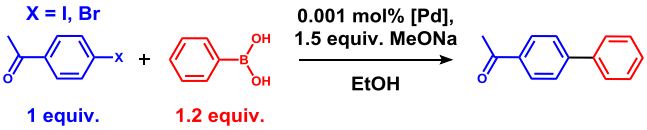

p-Halogenoacetophenone derivatives and phenylboronic acid were selected as substrates in order to easily distinguish between cross-coupling and homocoupling products. In all experiments, neither homocoupling of phenylboronic acids nor homocoupling of aryl halide or dehalogenation of *p*-halogenoacetophenone were observed. Thus, since the formation of 4-acetylbiphenyl was exclusive, we considered yields equal to conversion values.

In order to compare the effect of the nature of the ligands for the different catalysts, experiments were performed at different reaction temperatures measuring the catalytic performance. The results obtained were compared to those achieved using the Herrmann-Beller palladacycle precatalyst[32].

The evolution of the conversion of *p*-halogenoacetophenones with time was determined at 60°C and 25°C (Figures 3-4). Final conversions, Turnover numbers (TONs), Turnover-frequencies (TOFs), initial activities (iTOFs) and evolution of activities with their induction periods were determined for each reaction conditions and reported in Tables 1 and 2.

As a general trend, higher conversions were obtained with *p*-iodoacetophenone (Table 2), as expected from the respective C-X bond energies.[32]

First, for *p*-iodoacetophenone at 60°C (Figure 3, Table 1), complete conversions were achieved after 1 h in all cases. Figure 3 shows that, independently of ligand nature, the length of the bridging unit had an influence. For the three families of catalysts the longer the bridging chain is, the higher iTOFs are obtained. This effect is more pronounced for bisphosphine-based ligands where **C3a**, **C3b** and **C3c** exhibited iTOFs of 280, 1208 and 1830, respectively (Figure 3c, Table 1 entries 7-9). As expected, decreasing

the temperature to 25°C (Figure 4, Table 1) resulted in lower initial activities for all catalysts. Importantly, some

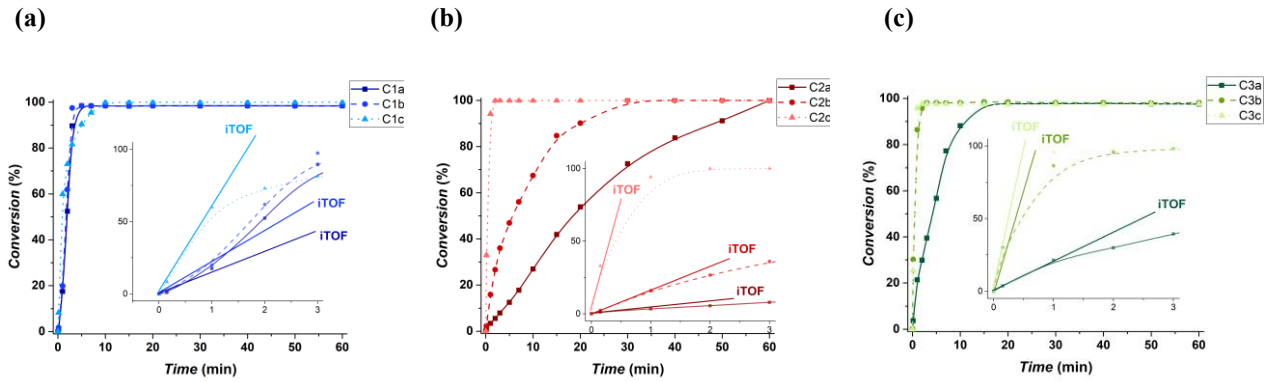

Figure 3. Conversion versus the time for the coupling reaction of *p*-iodoacetophenone with phenyl boronic acid using (a) **C1a-c**, (b) **C2a-c** and (c) **C3a-c** catalysts at 60°C.

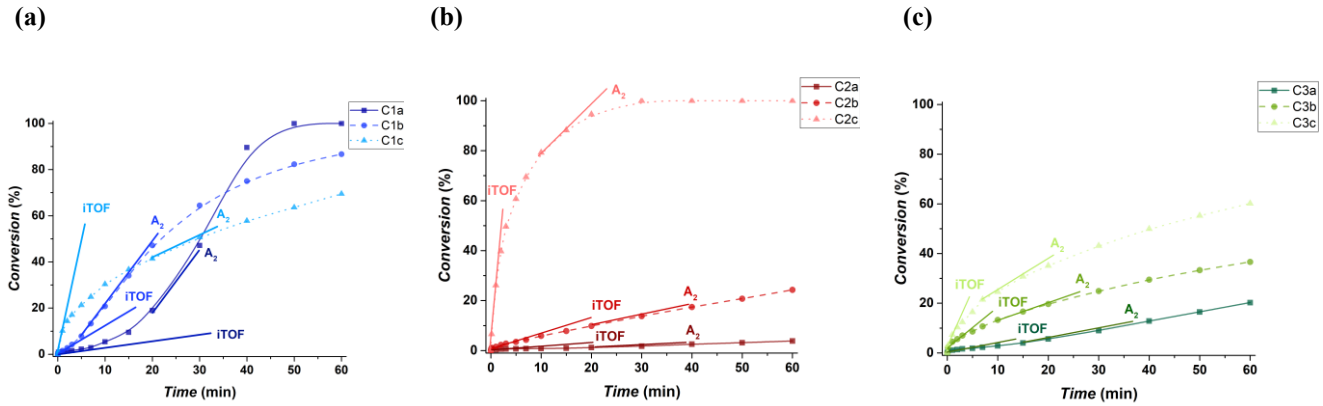

Figure 4. Conversion versus the time for the coupling reaction of *p*-iodoacetophenone with phenyl boronic acid using (a) **C1a-c**, (b) **C2a-c** and (c) **C3a-c** catalysts at 25°C.

Table 1. Catalyst Activities for the Suzuki-Miyaura Reaction of *p*-Haloacetophenone with Phenylboronic Acid.

Entry	Catalyst	*p*-iodoacetophenone				*p*-bromoacetophenone		
		60°C	25°C			60°C		
		iTOF (mol product · mol Pd^{-1} · min^{-1})	iTOF (mol product · mol Pd^{-1} · min^{-1})	A_2 (mol product · mol Pd^{-1} · min^{-1})	Induction time (min)	iTOF (mol product · mol Pd^{-1} · min^{-1})	A_2 (mol product · mol Pd^{-1} · min^{-1})	Induction time (min)
1	**C1a**	159	7	173	20	611	stopped	5
2	**C1b**	218	15	34	5	294	stopped	10
3	**C1c**	846	133	15	10	90	stopped	20
4	**C2a**	31	1	0.6	15	1	0.2	20
5	**C2b**	169	6	6	7	36	6	20
6	**C2c**	1337	318	66	7	206	stopped	5
7	**C3a**	280	5	3	15	108	16	20
8	**C3b**	1208	172	8	10	223	7	10
9	**C3c**	1830	229	6	7	240	22	10
10	**H-B**	106	3	26	20	254	stopped	20

8 x 10^{-4} mmol Pd, 0.8 mmol *p*-haloacetophenone, 1 mmol phenylboronic acid, 1.2 mmol MeONa and 9 x 10^{-2} mmol naphthalene as an internal standard in 16 mL absolute EtOH.

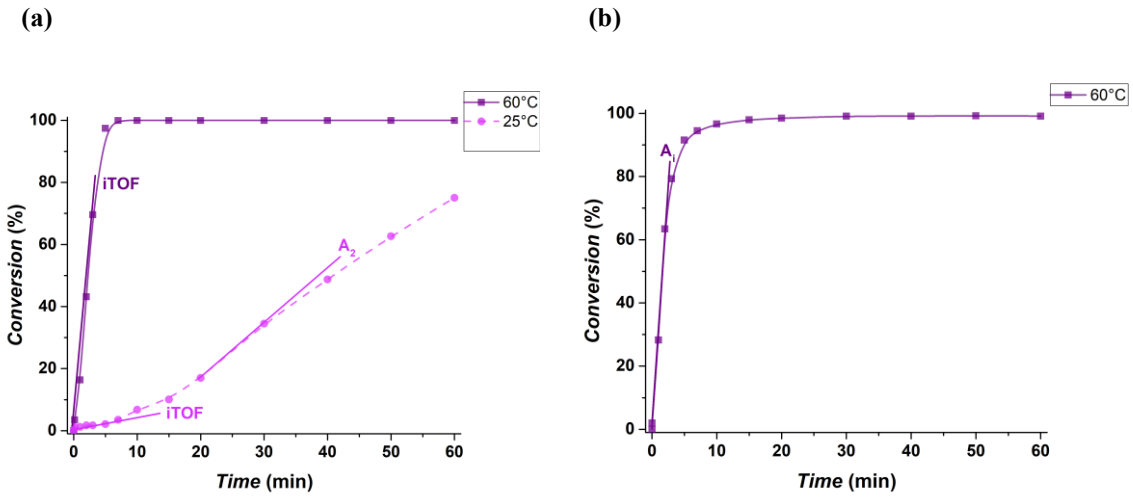

Figure 5. (a) Conversion versus the time for the coupling reaction of *p*-iodoacetophenone with phenyl boronic acid using the Herrmann-Beller catalyst at 60°C (purple) and at 25°C (pink). (b) Conversion versus the time for the coupling reaction of *p*-bromoacetophenone with phenyl boronic acid using the Herrmann-Beller catalyst at 60°C.

catalysts seem to evolve to different Pd-species since their catalytic activities (A_2) dramatically changed after some minutes at 25°C (Figure 4, Table 1). Remarkably, the kinetic curves for **C1a** and **C1b** catalysts demonstrate a sigmoid plot that indicates possible catalyst activation (Figure 4a). Thus, their catalytic activities increase with time while it decreases for **C1c**. As a result, since **C2a-c** and **C3a-c** follows the same trend observed at 60°C, higher conversions are achieved with smaller chelates for **C1a-c** (Figure 4a, Table 2 entries 1-3). Although, this phenomenon is not observed at 60°c maybe due to reaction running too fast, it can be inferred that the different catalytic performance of **C1a-c** complexes at 25°C reveals a crucial role of NHC ligands.

Evolution of Pd species during the catalytic reactions. Recently, Astakhov *et al.*[33] demonstrated the formation of Pd NPs when molecular Pd complexes with NHC ligands are used in the Mizoroki-Heck reaction. In our case, TEM analyses of the reaction after catalytic runs show the presence of Pd NPs for all **C1a-c** catalysts (Figure 7 and Table S3). Two families of Pd NPs of *ca.* 3.7 ± 1.1 and 11.6 ± 1.8 nm could be found for **C1a**, a single family of *ca.* 10.6 ± 1.6 nm for **C1b** and two families of *ca.* 9.8 ± 2.3 and 63.1 ± 11.9 nm for **C1c**. Thus, size-dependent catalytic activity of the evolved Pd NPs from **C1a-c** can be rationalized: increased catalytic activities is observed with decreasing NPs size.

Additionally, the **C2a-c** complexes evolved to Pd NPs under turnover conditions exhibiting higher iTOFs for smaller nanoparticles (Figure S43, Tables 1 and S3).

Contrary to **C1a-c** and **C2a-c**, Pd NPs evolved from **C3a-c** complexes (Figure S43 and Table S1) exhibited higher activities for larger NPs sizes. This can be explained by the different coordination modes of the ligands at the Pd NPs surface. On the one hand, carbene and pyridyl -based ligands of **C1a-c** and **C2a-c** can stabilize nanoparticles both by σ- and π- interactions.[34] More to this point, metal-to-carbene π-backdonation can be responsible for up to 20-30% of total M-to-C bond strength in transition metal-NHC entities.[35-37] On the other hand, although **C3a-c** exhibit both σ-donation and π-backdonation like carbene-based ligands, they present a lower binding ability. Then, since all bisphosphine ligands in **C3a-c** exhibit similar Tolman's cone angles,[38] when increasing the bridge length, the bite angle becomes wider while stabilizing nanoparticles because of their extended conformation and further coordination to long-in-distance separate Pd atoms.[39] This may tune both electronic and steric properties at the NPs surface and consequently the catalytic behavior.

TEM analyses of reaction mixture obtained at 60°C for the same substrate revealed smaller NPs for **C1a-c** and **C2a-c** but larger for **C3a-c** complexes (Figure S42, Tables 1 and S3). Thus, increasing the temperature could greatly enhance the complex decomposition followed by cluster formation as well as favoring the leaching of highly-active Pd species from Pd NPs.

Interestingly, the new **C1a-c** catalysts prepared here exhibited higher initial activities than that of the Herrmann-Beller palladacycle catalyst (Table 1 and Table 2). Figure 5 shows that the palladacycle exhibit an enhanced activity after 20 min of reaction at 25°C. As already evidenced by Louie *et al.*[40] during Heck reaction, the palladacycle was transformed into Pd NPs explaining such an observation (Figures S42-S44 and Table S3).

When *p*-bromoacetophenone was used as substrate, complete conversions where only obtained with **C1a** and the Herrmann-Beller catalysts (Table 2 entries 1 and 10).

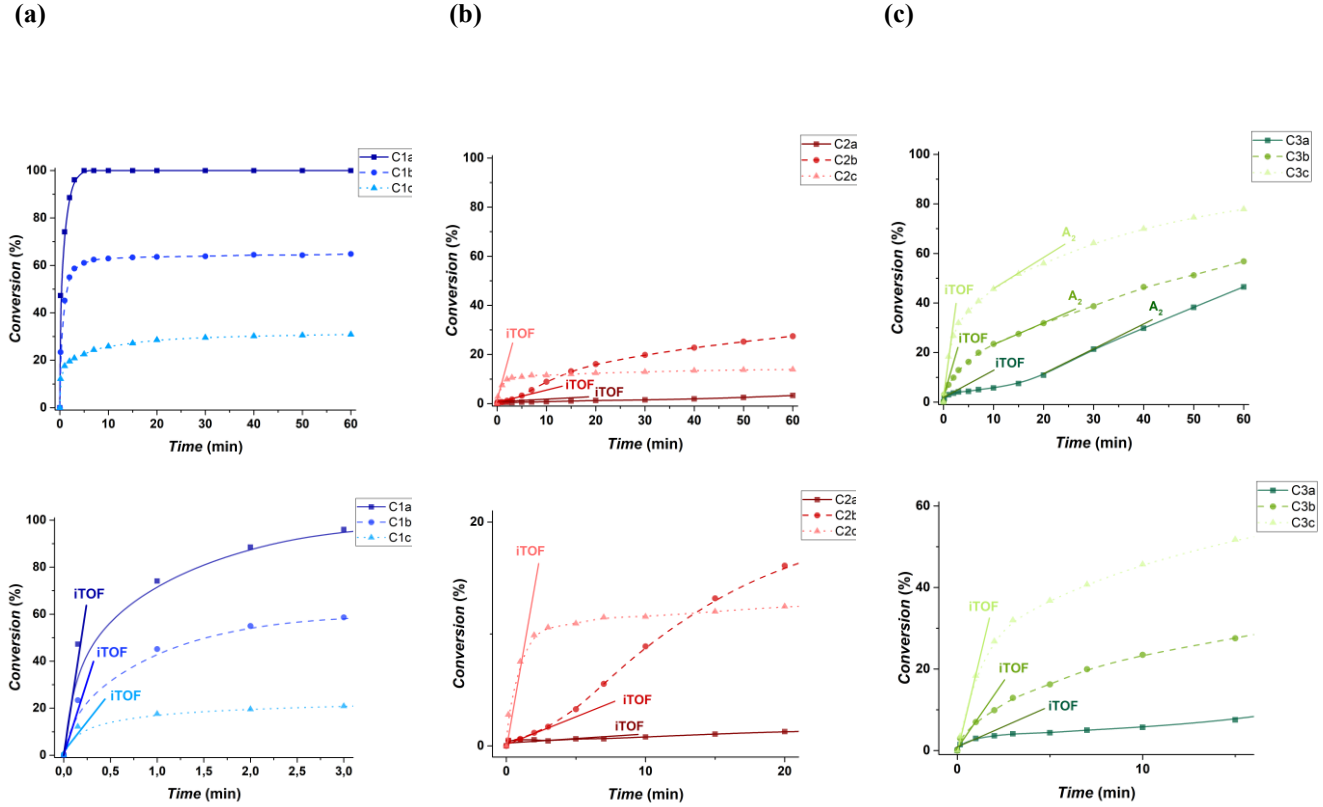

Figure 6. Conversion versus the time (top) and insets (bottom) for the coupling reaction of *p*-bromoacetophenone with phenyl boronic acid using (a) **C1a-c**, (b) **C2a-c** and (c) **C3a-c** catalysts at 25°C.

Table 2. Conversion, TON and TOF Values for the Suzuki-Miyaura Reaction of *p*-Haloacetophenone with Phenylboronic Acid.

Entry	Catalyst	*p*-iodoacetophenone						*p*-bromoacetophenone		
		60°C			25°C			60°C		
		Conv.	TON	TOF (h^{-1})	Conv.[b]	TON	TOF (h^{-1})	Conv.[b]	TON	TOF (h^{-1})
1	**C1a**	100	1000	12000	100	1000	1200	100	1000	12000
2	**C1b**	100	1000	20000	87	867	867	65	648	3888
3	**C1c**	100	1000	6000	70	695	695	31	309	927
4	**C2a**	100	1000	1000	4	39	39	3	331	331
5	**C2b**	100	1000	2000	24	243	243	28	275	275
6	**C2c**	100	1000	30000	100	100	2000	14	139	417
7	**C3a**	100	1000	4000	20	203	203	47	465	465
8	**C3b**	100	1000	20000	37	366	366	57	568	568
9	**C3c**	100	1000	60000	60	602	602	78	779	779
10	**H-B**	100	1000	8571	75	750	750	99	991	2973

8×10^{-4} mmol Pd, 0.8 mmol *p*-haloacetophenone, 1 mmol phenylboronic acid, 1.2 mmol MeONa and 9×10^{-2} mmol naphthalene as an internal standard in 16 mL absolute EtOH. Conversion after 1 h reaction

Here, the three families of catalysts showed different trends. Firstly, **C1a-c** catalysts reached a plateau in the conversion in the first 5-20 minutes with highest iTOFs for smallest chelates (Figure 6a, Table 1 entries 1-3). In contrast with *p*-iodoacetophenone, TEM analyses reveal the formation of homogenous spherical Pd NPs (Figure 7 and Table S3) for the three catalysts and, as evidenced from their size distribution histograms, larger particles are formed for longer bridges. Although this could explain their initial iTOFs, their depletion remains raveled. As the solid surface is modified with the time (*i.e.* clusterification step), the loss of activity could be due to the surface rearrangement or the

Table 3. Conversion, TON and TOF Values for the Suzuki-Miyaura Reaction of *p*-Haloacetophenone with Phenylboronic Acid in the Presence of Hg.

Entry	Catalyst	*p*-iodoacetophenone			*p*-bromoacetophenone		
		25°C			60°C		
		Conv.	TON	TOF (h^{-1})	Conv.	TON	TOF (h^{-1})
1	**C1a**	4	38	38	58	580	580
2	**C1b**	29	289	289	14	137	137
3	**C1c**	22	218	218	6	58	58
4	**C2a**	1	10	10	1	8	8
5	**C2b**	6	60	60	7	69	69
6	**C2c**	19	193	193	2	25	25
7	**C3a**	1	10	10	5	49	49
8	**C3b**	1	9	9	1	13	13
9	**C3c**	1	14	14	1	16	16
10	**H-B**	3	33	33	1	10	10

8×10^{-4} mmol Pd, 0.8 mmol *p*-haloacetophenone, 1 mmol phenylboronic acid, 1.2 mmol MeONa, 2 mmol Hg, and 9×10^{-2} mmol naphthalene as an internal standard in 16 mL absolute EtOH. Conversion after 1 h reaction.

degradation of Pd NPs stabilizers entities (decomposition of ligands or *in situ* generated species).

Secondly, as observed for *p*-iodoacetophenone, **C2a-c** and **C3a-c** catalysts exhibited higher iTOFs for longer bridges but **C2c** activity stopped after 5 minutes.

Finally, data clearly indicates that **C1a** is more active than any other catalyst because of its faster kinetics (Table 1 entries 1 and 10). Given these catalytic evidences, it can be inferred that the catalyst performance is depending on the ligand scaffold and its nature, as well as the targeted aryl halide to be coupled. However, the nature of the active species remains unraveled. All data obtained with the three complex series are compiled in Table 2.

Elucidating the nature of active species. Mercury poisoning tests[40] were applied to the reactions of *p*-iodoacetophenone and *p*-bromoacetophenone with phenylboronic acid under catalysis conditions with all complexes. A large excess of Hg(0) (Hg:Pd ≈ 2000:1 mol/mol) was added to the reaction mixtures at the beginning. As shown in Table 2 and Table 3, the catalytic reactions ceased completely for all catalysts but some conversions were observed with **C1b**, **C1c** and **C2c** when using *p*-iodoacetophenone as substrate. Similar results were observed when using *p*-bromoacetophenone. In this case, conversions completely ceased for all catalysts despite some conversions with **C1a** and **C1b** (Table 3).

These data suggest that molecular complexes act in fact as precatalysts and their evolved Pd NPs act as the active species or as reservoir of molecular palladium species. Then, the conversions observed for the catalyst could be due to (a) the high activity of their evolved Pd NPs before Hg-Pd amalgam formation or (b) the generation of highly-active catalytic species. All these analyses are in accordance with the different results observed in catalysis depending on the molecular or colloidal nature of the introduced catalysts.

However, the mercury poisoning tests is not a definitive proof since the amalgam of Hg and Pd from the NPs could prevent potential Pd molecular species from leaching.[42]

TEM analyses, mercury poisoning tests and catalytic studies suggest that the key role of Pd clusters could be highlighted as "cocktail"-type behavior.[34]

These results prompted us to investigate the process of evolution of **C1a-c** pre-catalysts whose exhibited moderate conversions in the presence of Hg and catalyst depletion when reacting with *p*-bromoacetophenone (Table 3).

Although NHC-based ligands are well known because of their stabilizing features under oxidative conditions, it was evidenced that Pd-NHC complexes can evolve through the cleavage of the Pd-$C_{carbene}$ bond by a C-C reductive elimination from the intermediate after the oxidative addition of aryl halides.[34] Thus, we attempted to determine the products formed during the transformation of the **C1a-c** complexes over the course of the Suzuki-Miyaura reaction. A dedicated study of the reaction between *p*-iodoacetophenone was performed using 0.5 equivalents of catalyst precursor **C1a-c** in the presence of 3 equivalents of MeONa. Although the formation of Pd NPs was evidenced for the three complexes of C1 family after catalytic tests (*vide supra*), Pd black formation was only observed when using **C1a** and **C1b** under these conditions. After separation of Pd black, the crude solutions were analyzed by MS-ESI (Figures S22-S24). In all cases,

no peaks attributed to the reductive elimination of the ligand and the

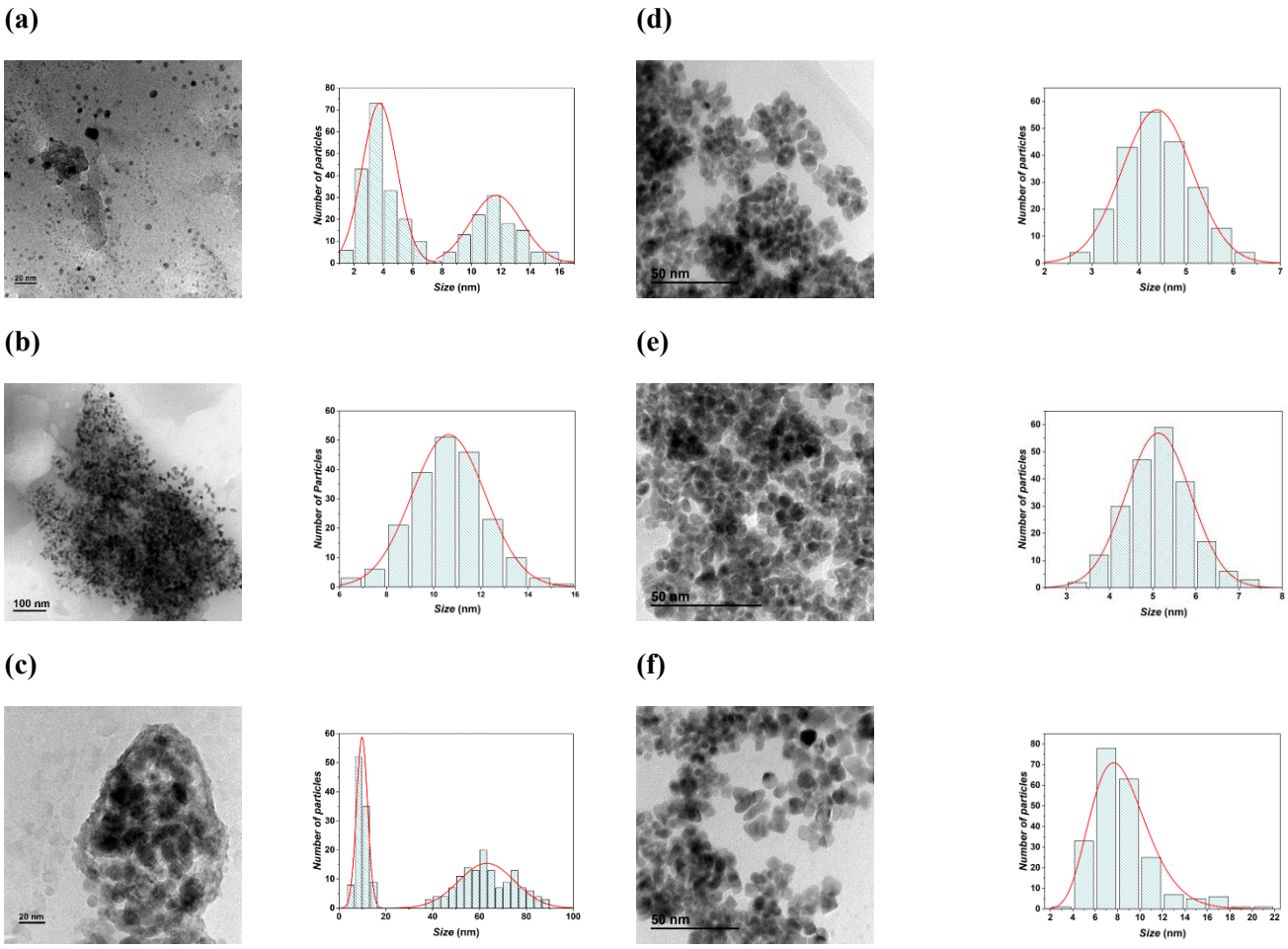

Figure 7. TEM micrographs and the corresponding size-histograms of Pd NPs observed after the catalytic tests with *p*-iodoacetophenone as substrate at 25°C using (a) **C1a**, (b) **C1b** and (c) **C1c**. TEM micrographs and the corresponding size-histograms of Pd NPs observed after the catalytic tests with *p*-bromoacetophenone as substrate at 60°C using (d) **C1a**, (e) **C1b** and (f) **C1c.**

substrate were detected but double-charged species for **C1a** and **C1b** at m/z = 385.1533 and 399.1676, respectively (Figures S22-S23). We found that these peaks can be attributed to $[Pd(bisNHC)_2]^{2+}$ homoleptic tetracarbene species (Figures S25-S26). These cationic species were confirmed by independent synthesis according to Scheme 3 (Figures S36-S41) revealing an excellent agreement with observed fragmentation patterns in the MS-ESI spectra. Contrary to the assumption of strong M-NHC binding, these transformations are a clear demonstration of a controlled cleavage of the M-NHC bond, which could be a pivotal step for high-performance palladium catalysis.

On the basis of the obtained results and the good fit of their simulated ESI-MS spectra, we postulated that the reduction of these complexes followed by the oxidative addition of the aryl halide resulted in the formation of ionic species as proposed by Górna *et al.*[43] Such species can act as stabilizers of their first evolved Pd NPs (oxidative addition step) as well as a reservoir source enhancing catalyst turnover. In fact, very recently, Eremin *et al.*[44] evidenced the formation of anionic palladium species in the Mizoroki-Heck reaction. However, no evidences of these anionic palladium species were observed in our case (Figures S27-S29).

Scheme 3. Synthetic Pathway for C1aa and C1bb Complexes

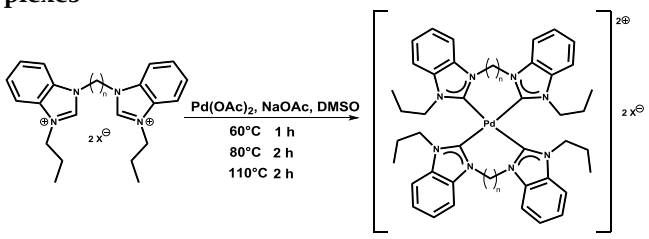

3a: n = 1 X = I
3b: n = 2 X = Br

C1aa: n = 1 X = I 15%
C1bb: n = 2 X = Br 27%

Interestingly, the same results were observed when using *p*-bromoacetophenone (Figures S30-S35). Thus, the presence of the **C1aa** and **C1bb** double-charged cationic species generated from their respective **C1a** and **C1b**

Scheme 4. Catalyst Evolution and Cationic Pd Species-Stabilized "Cocktail"-Type Mode of Suzuki-Miyaura Reaction with a Pd-bisNHC Catalyst Precursor.

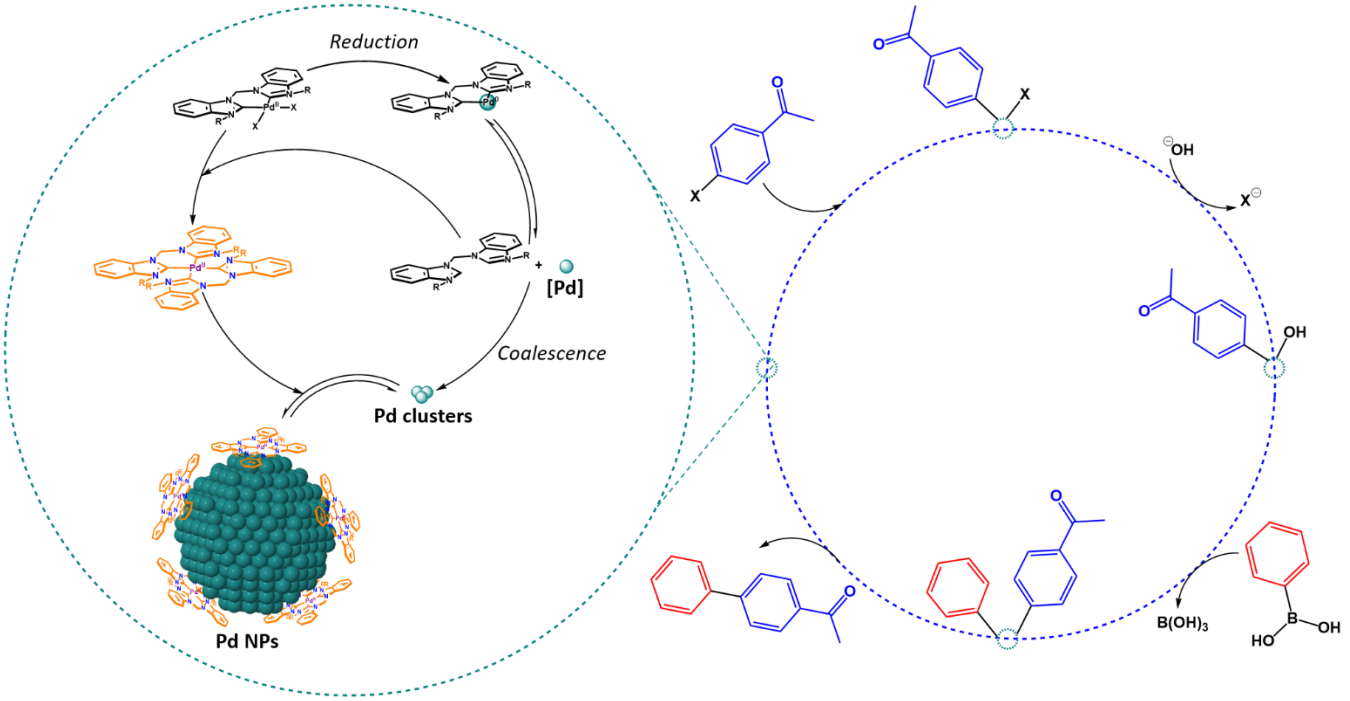

complexes could be explained through their enhanced formation by the pseudo-agostic and agostic interactions between the bridge –CH_2- protons and the palladium core (*vide supra*). From here, we propose a mechanism (Scheme 4) in which "bisNHC-free" metal species are released from the [PdX_2(bisNHC)] precursors.

Since these Pd species start to coalesce, the free bisNHC can react with the precursor under catalytic conditions to yield $[Pd(bisNHC)_2]^{2+}$ species. Thus, it could be expected that the homoleptic tetracarbene species govern the stabilization of evolving Pd NPs.

It is important to note that the catalytic performance of these systems strongly depends on the stability of Pd NPs against further aggregation to inactive Pd black. Then, the catalyst depletion experienced by **C1b** and **C1c** complexes when using *p*-bromoacetophenone (*vide supra*) could be attributed to the degradation of **C1bb** mediated by the catalytic conditions for the former and the absence of $[Pd(bisNHC)_2]^{2+}$ species for the latter.

■ CONCLUSIONS

In conclusion, we have prepared and characterized a new series of NHC-based Pd(II) complexes as catalysts for the Suzuki-Miyaura reaction. Generally, in the presence of these catalysts, all reactions are carried out with good to excellent yields, and some quantitative yields can be achieved for aryl *p*-bromoacetophenone and *p*-iodoacetophenone. Moreover, most of the TOF values obtained for both *p*-iodoacetophenone and *p*-bromoacetophenone reactivity exceeded that obtained in the presence or the Herrmann-Beller catalysts reaching up to 12000 h^{-1} at 0.1% catalyst loading under environmentally friendly and mild conditions.

We have demonstrated for the first time, a structure-activity relationship for palladium(II) complexes bearing bisNHC, bispyridyl and bisphosphine ligands in the Suzuki-Miyaura reaction. Firstly, Pd-release in the bulk media can be controlled by the nature of the selected bidentate ligands: an easier decoordination for bisphosphine ligands towards Pd NPs formation was observed compared to palladium(II) complexes bearing bispyridyl and even bisNHC ligands under same reaction conditions. Secondly, in general, longer bridges enhance overall catalyst performance but for bisNHC-based catalysts, shorter bridges are the responsible for catalyst performance enhancement. The catalytic studies, TEM analyses and mercury poisoning tests revealed that these enhanced catalytic activities could be ascribed to the formation of Pd NPs. Interestingly for **C1a** and **C1b** complexes, we evidenced that they initially evolved to $[Pd(bisNHC)_2]^{2+}$ species, which are proposed to be pivotal species involved in the catalytic cycle as NPs stabilizers and/or reservoir sources enhancing activities. A possible mechanism of the chemical transformation of the [PdX_2(bisNHC)] complexes and formation of their corresponding homoleptic tetracarbene species is therefore presented here. Thirdly, it was also found that increasing the temperature could greatly enhance the initial catalytic activities due to a faster complex decomposition and further clusterification. Finally, the nature of the substrate has a strong influence in the

catalytic activity since not only the C-Br bond is more difficult to activate, as expected, but also it controls the size and shape of evolved Pd NPs upon clusterification, playing as well a role in stabilization of formed Pd NPs.

These results will provide a new guideline for the design and applications of new catalysts. Upcoming work based on controlling the generation of expected highly-active catalytic moieties from **C1a-c** catalyst clusterification is under progress. More studies on the subject are anticipated in the near future to evaluate the stabilization of Pd NPs by tetracarbene homoleptic complexes.

■ EXPERIMENTAL SECTION

Materials and Methods. GC analyses were performed on a Shimadzu Nexis GC-2030 gas chromatograph equipped with a FID detector, a HP-5 column (cross-linked 5% phenylmethylsiloxane, 30 m × 0.25 mm i.d. × 0.25 µm film thickness) with hydrogen as carrier gas. Yields were determined by GC based on the relative area of GC-signals referred to an internal standard (naphthalene) calibrated to the corresponding pure compounds.

Infrared (IR) spectra were recorded with a Thermo Scientific Nicolet iS5 spectrometer in the range 4000-525 cm^{-1} in attenuated total reflectance (ATR) mode.

^{1}H NMR, ^{13}C NMR, $^{31}P\{^{1}H\}$ NMR, HSQC and HMBC spectra were recorded on an Bruker Avance III 400 spectrometer at a temperature of 25°c. All chemical shift values are given in ppm.

The palladium content was determined using a ICP-OES ACTIVA Jobin Yvon spectrometer from a solution obtained by treatment of the catalysts with sulfuric acid and aqua regia in a Teflon reactor at 400-450°C.

Electrospray ionization Mass Spectrometry (ESI-MS) experiments were performed on a Bruker QTOF Impact II –instrument equipped with an UHPLC U3000 – Dionex by the Centre Commun de Spectrométrie de Masse from the University of Lyon.

Transmission electron microscopy (TEM) analyses were carried out on a JEOL 2010 microscope with an instrumental magnification of 50000x to 1000000x and an acceleration voltage of 200kV. The point-to-point resolution of the microscope was 0.19 nm and the resolution between the lines was 0.14 nm. The microscope is equipped with an EDX link ISIS analyzer from Oxford instruments. Energy dispersive X-ray microanalysis (EDX) was conducted using a probe size 25-100 nm to analyze grains of the phases. The size distributions were determined via manual analysis of enlarged micrographs by measuring ca. 200 particles on a given grid to obtain a statistical size distribution and a mean diameter.

Crystals for the solid-state structures of the palladium **C1a-c** complexes could be obtained by slow evaporation of saturated solutions of the complexes in DMF or DMSO. Suitable single crystals were mounted on a nylon loop in perfluoroether oil on an Xcalibur, Atlas, Geminis ultra diffractometer. The crystals were keep at a steady T = 150.01(10) K during data collection. Data were measured using ω scans using MoK_{α} radiation. The total number of runs and images was based on the strategy calculation from the program CrysAlisPro.[43] The structures were solved with the SheIXT[44] structure solution program using Intrinsic Phasing solution method and by using Olex2[45] as a graphical interface. The models were refined with version 2018/3 of SheIXL using Least Squares minimization. All non-hydrogen atoms were refined anisotropically. Hydrogen atom positions were calculated geometrically and refined using the riding model.

Catalytic Performance Studies for the Suzuki-Miyaura Reaction. In glass tubes of a Radleys Carousel 12 Plus Station™ fitted with a water-cooled aluminum reflux head and septa, 16 mL of an absolute ethanol solution containing *p*-halogenoacetophenone (0.05 M), phenylboronic acid (0.06 M) and MeONa (0.075 M) were added. The reaction mixtures were stirred and heated at 60°C or 25°C under nitrogen atmosphere for 30 minutes. Thus, the palladium catalyst (8×10^{-4} mmol Pd) was added from a stock solution/suspension of the former. The mixture was vigorously stirred and kept at 60°C for 1 h under nitrogen. Then, an aliquot (*ca.* 0.5 mL) of the reaction crude was taken at different reaction times and quenched in a vial filled with water/ethyl acetate mixture (2:1.5, 3.5 mL) and with naphthalene (0.09 mmol) as standard. The organic phase was analyzed by GC and GC-MS. For TEM analyses, a drop of the crude mixture was deposited under the holey carbon-covered copper.

Synthesis and Characterization of the Ligands

1-propylbenzimidazole (*2*). A mixture of benzimidazole (8.86 g, 75 mmol, 1 eq), bromopropane (6.83 mL, 75 mmol, 1 eq) and potassium carbonate (20.73 g, 150 mmol, 2 eq) were refluxed in acetone (40 mL) overnight. After cooling to room temperature, the reaction mixture was filtered. The product was obtained as a yellow oil after removing the organic phase under reduced pressure. Yield: 10.42 g. 87%. The spectroscopic data are in accordance with that reported in the literature.[48]

1,1'-Dipropyl-3,3'-methylenebisbenzimidazolium diiodide (*3a*). In a sealed tube, a mixture of 1-propylbenzimidazole (1000 mg, 6.2 mmol, 2.1 eq) and diiodomethane (240 µL, 3.0 mmol, 1 eq) was heated at 120°C for 4 h. After cooling to room temperature, acetonitrile (5 mL) was added to crush the solid by sonication. The crude precipitate was filtered off and washed with acetonitrile (5 mL x 2). The product was obtained as a pale white powder. Yield: 900 mg, 52%. ^{1}H NMR (DMSO-d_6, 400 MHz, 25°C) δ 0.97 (t, *J*

= 7.03 Hz, 6H, H_4), 1.97 (m, 4H, H_3), 4.55 (t, *J* = 7.00 Hz, 4H, H_2), 7.40 (s, 2H, H_{11}), 7.79 (m, 4H, H_7 and H_8), 8.19 (d, *J* = 7.94 Hz, 2H, H_9), 8.39 (d, *J* = 8.23 Hz, 2H, H_6), 10.31 (s, 2H, H_1). $^{13}C\{^1H\}$ NMR (DMSO-*d*$_6$, 100 MHz, 25°C) δ 11.1 (C_4), 22.4 (C_3), 49.1 (C_2), 55.6 (C_{11}), 114.1 (C_6), 114.7 (C_9), 127.6 (C_7), 127.9 (C_8), 131.0 (C_{10}), 131.6 (C_5), 144.2 (C_1). (ATR) cm^{-1}: 1559 (ν(C=C), ν(C=N))ar, 1431 (δ(C=C), δ(C=N))ar, 1014 δ(C-H)ip, 751 δ(C-H)oop. HRMS-ESI (DMSO): *m*/*z* = 461.1188 ($[M-I]^+$).

1,1'-Dipropyl-3,3'-(1,2-dimethylene)bisbenzimidazolium dibromide (*3b*). In a sealed tube, a mixture of 1-propylbenzimidazole (641 mg, 4 mmol, 2 eq) and 1,2-dibromoethane (172 µL, 2.0 mmol, 1 eq) was heated at 120°C for 4 h. After cooling to room temperature, acetonitrile (5 mL) was added to crush the solid by sonication. The crude precipitate was filtered off and washed with acetonitrile (5 mL x 2). The product was obtained as a pale white powder. Yield: 806 mg, 79%. ^1H NMR (D_2O, 400 MHz, 25°C) δ 0.82 (t, *J* = 7.29 Hz, 6H, H_4), 1.85 (m, 4H, H_3), 4.41 (t, *J* = 7.25 Hz, 4H, H_2), 5.24 (s, 4H, H_{11}), 7.38 (d, *J* = 8.67 Hz, 2H, H_5), 7.55 (t, *J* = 8.14 Hz, 2H, H_7), 7.68 (t, *J* = 7.91 Hz, 2H, H_6), 7.90 (d, *J* = 8.33 Hz, 2H, H_8), 9.41 (s, 2H, H_1). $^{13}C\{^1H\}$ NMR (D_2O, 100 MHz, 25°C) δ 10.1 (C_4), 22.0 (C_3), 46.4 (C_{11}), 49.0 (C_2), 111.6 (C_5), 113.9 (C_8), 127.6 (C_6), 127.7 (C_7), 131.0 (C_9), 131.2 (C_{10}), 141.1 (C_1). (ATR) cm^{-1}: 3012 ν(C-H)ar, 2938 ν(C-H), 1565 (ν(C=C), ν(C=N))ar, 1431 (δ(C=C), δ(C=N))ar, 1014 δ(C-H)ip, 751 δ(C-H)oop. HRMS-ESI (DMSO): *m*/*z* = 427.1481 ($[M-Br]^+$), 174.1145 ($[M-2Br]^{+2}$).

1,1'-Dipropyl-3,3'-(1,3-trimethylene)bisbenzimidazolium diiodide (*3c*). In a sealed tube, a mixture of 1-propylbenzimidazole (801 mg, 5 mmol, 2 eq) and 1,3-diiodopropane (287 µL, 2.5 mmol, 1 eq) was heated at 130°C for 30 min. After cooling to room temperature, acetonitrile (5 mL) was added to crush the solid by sonication. The crude white precipitate was filtered off and washed with acetonitrile (5 mL x 2). The product was obtained as a crude white powder. Yield: 1062 mg, 69%. ^1H NMR (DMSO-*d*$_6$, 400 MHz, 25°C) δ 0.97 (t, *J* = 7.39 Hz, 6H, H_{14}), 1.94 (m, 4H, H_{13}), 2.65 (m, 2H, H_{11}), 4.47 (t, *J* = 7.10 Hz, 4H, H_{12}), 4.69 (t, *J* = 7.29 Hz, 4H, H_{10}), 7.73 (m, 4H, H_1 and H_5), 8.13 (m, 4H, H_2 and H_5), 9.81 (s, 2H, H_8). $^{13}C\{^1H\}$ NMR (DMSO-*d*$_6$, 100 MHz, 25°C) 11.1 (C_{14}), 22.8 (C_{13}), 28.4 (C_{11}), 44.4 (C_{10}), 48.7 (C_{12}), 114.1 (C_5), 114.3 (C_2), 127.1 (C_6), 127.2 (C_1), 131.5 (C_4), 131.6 (C_3), 142.7 (C_8). (ATR) cm^{-1}: 1565 (ν(C=C), ν(C=N))ar, 1431 (δ(C=C), δ(C=N))ar, 1014 δ(C-H)ip, 751 δ(C-H)oop. HRMS-ESI (DMSO): *m*/*z* = 489.1497 ($[M-I]^+$).

Synthesis and Characterization of the Complexes**Diiodido-(1,1'-dipropyl-3,3'-methylenedibenzimidazolin-2,2'-diylidene)palladium(II) (*C1a*).** Palladium(II) acetate (79 mg, 0.35 mmol, 1 eq) and ligand **3a** (210 mg, 0.36 mmol, 1.01 eq) were dissolved in degassed DMSO (3 mL) in a round-bottom flask. The reddish mixture was stirred for 4 h at room temperature, 17 h at 40°C and, finally, 2 h at 120°C. After cooling to room temperature, a yellow suspension was obtained. Filtration of the reaction mixture yielded the product as a greenish powder. Yield: 150 mg, 61%. ^1H NMR (DMSO-*d*$_6$, 400 MHz, 25°C): δ 0.83 (t, *J* = 6.4 Hz, 6H, H_4), 1.89 (m, 4H, H_3), 4.43 (m, 2H, H_2), 4.97 (m, 2H, H_2), 6.78 (d, *J* = 14.2 Hz, 1H, H_{11}), 7.45 (m, 5H, H_7, H_8 and H_{11}), 7.81 (d, *J* = 7.9 Hz, 2H, H_9), 8.27 (d, *J* = 7.9 Hz, 2H, H_6); $^{13}C\{^1H\}$ NMR (DMSO-*d*$_6$, 100 MHz, 25°C): δ 11.36 (C_4), 22.92 (C_3), 50.68 (C_2), 58.20 (C_{11}), 111.74 (C_6), 112.61 (C_9), 124.60 (C_7), 124.82 (C_8), 133.23 (C_5) 133.88 (C_{10}). IR (ATR) cm^{-1}: 3033 ν(C-H)ar, 2966 ν(C-H), 1414, 1388 (δ(C=C), δ(C=N))ar, 1040, 1014 δ(C-H)ip, 751 δ(C-H)oop. HRMS-ESI (DMSO): *m*/*z* = 714.9020 ($[M+Na]^+$), 565.0075 ($[M-I]^+$). Note: C1, C2 and C11 are not observed in 1D. C11 and C2 are observed in HSQC.

Dibromido-(1,1'-dipropyl-3,3'-ethylenedibenzimidazolin-2,2'-diylidene)palladium(II) (*C1b*). Palladium(II) acetate (109 mg, 0.48 mmol, 1 eq) and ligand **3b** (250 mg, 0.49 mmol, 1.01 eq) were dissolved in degassed DMSO (3 mL) in a round-bottom flask. The reddish mixture was stirred for 4 h at room temperature, 17 h at 40°C and, finally, 2 h at 120°C. After cooling to room temperature, a greenish suspension was obtained. Filtration of the reaction mixture yielded the product as a pale yellow powder. Yield: 275 mg, 92%. ^1H NMR (DMSO-*d*$_6$, 400 MHz, 25°C): δ 0.98 (t, *J* = 7.2 Hz, 6H, H_4), 1.88 (m, 2H, H_3), 2.06 (m, 2H, H_3), 4.51 (m, 2H, H_2), 4.83 (m, 2H, H_2), 5.10 (m, 2H, H_{10}), 5.65 (m, 2H, H_{10}), 7.38 (m, 4H, H_7 and H_7), 7.75 (m, 4H, H_5 and H_8); $^{13}C\{^1H\}$ NMR (DMSO-*d*$_6$, 100 MHz, 25°C): δ 11.50 (C_4), 22.94 (C_3), 44.37 (C_{10}), 50.64 (C_2), 111.68 (C_5), 111.99 (C_8), 124.01 (C_6), 124.24 (C_7), 133.95 (C_{11}), 134.24 (C_9). (ATR) cm^{-1}: 3032 ν(C-H)ar, 2952 ν(C-H), 1443, 1390 (δ(C=C), δ(C=N))ar, 1053, 1013 δ(C-H)ip, 748 δ(C-H)oop. HRMS-ESI (DMSO): *m*/*z* = 634.9433 ($[M+Na]^+$), 533.0358 ($[M-Br]^+$). Note: C1 is not observed

Diiodido-(1,1'-dipropyl-3,3'-propylenedibenzimidazolin-2,2'-diylidene)palladium(II) (*C1c*). Palladium(II) acetate (180 mg, 0.80 mmol, 1 eq) and ligand **3c** (500 mg, 0.81 mmol, 1.01 eq) were dissolved in degassed DMSO (3 mL) in a round-bottom flask. The reddish mixture was stirred for 4 h at room temperature, 17 h at 40°C and, finally, 2 h at 120°C. After cooling to room temperature, a yellowish suspension was obtained. Filtration of the reaction mixture yielded the product as a pale yellow powder. Yield: 345 mg, 60%. ^1H NMR (DMSO-*d*$_6$, 400 MHz, 25°C): δ 1.09 (t, *J* = 7.5 Hz, 6H, H_9), 1.80 (m, 2H, H_8), 1.99 (m, 1H, H_{11}), 2.15 (m, 2H, H_8), 2.62 (m, 1H, H_{11}), 4.51 (td, *J* = 4.79 Hz, *J* = 12.76 Hz, 2H, H_7), 4.74 (td, *J* = 5.19 Hz, *J* = 12.89 Hz, 2H, H_7), 4.88 (dd, *J* = 5.09 Hz, *J* = 14.90 Hz, 2H, H_{10}), 5.23 (dd, *J* = 11.94 Hz, *J* = 14.50 Hz, 2H, H_{10}), 7.30 (m, 4H, H_2 and H_5), 7.69 (m, 4H, H_1 and H_6); $^{13}C\{^1H\}$ NMR (DMSO-*d*$_6$, 100 MHz, 25°C): δ 11.11 (C_9), 21.37 (C_8), 29.30 (C_{11}), 48.82 (C_{10}), 50.24 (C_7), 110.7 (C_1), 111.7 (C_6), 123.20 (C_2), 123.40 (C_5), 133.12 (C_3), 134.04 (C_4). (ATR) cm^{-1}: 3033 ν(C-H)ar, 2938 ν(C-H), 1455, 1402 (δ(C=C), δ(C=N))ar, 1044, 1027 δ(C-

H)ip, 742 δ(C-H)oop. HRMS-ESI (DMSO): m/z = 742.9328 ($[M+Na]^+$), 593.0384 ($[M-I]^+$). Note: C12 is not observed

Bis(1,1'-dipropyl-3,3'-methylenedibenzimidazolin-2,2'-diylidene)palladium(II) iodide (*C1aa*). Palladium(II) acetate (29 mg, 0.13 mmol, 1 eq), ligand **3a** (163 mg, 0.28 mmol, 2.1 eq) and sodium acetate (21.6 mg, 0.26 mmol, 2 eq) were dissolved in degassed DMSO (3 mL) in a round-bottom flask. The brownish mixture was stirred for 1 h at 60°C, 2 h at 80°C and 1 h at 110°C. Thus, sodium acetate (21.6 mg, 0.26 mmol, 2 eq) was added again and the reaction mixture was kept at 110°C for 1.5 h. After cooling to room temperature, a yellowish suspension was obtained. Water (6 mL) was added to precipitate a pale yellow powder. The precipitate was filtered and washed with acetone (6 mL x 6). The product was obtained as a white powder. Yield: 20 mg, 15%. ^{1}H NMR (DMSO-d_6, 400 MHz, 25°C): δ 0.54 (t, J = 7.21 Hz, 12H, H_4), 1.54 (m, 4H, H_3), 1.76 (m, 4H, H_3), 3.60 (m, 4H, H_2), 4.33 (m, 4H, H_2), 7.00 (d, J = 14.49 Hz, 2H, H_{11}), 7.51 (t, J = 7.82 Hz, 4H, H_7), 7.62 (t, J = 8.09 Hz, 4H, H_8), 7.64 (d, J = 14.03 Hz, 2H, H_{11}), 7.86 (d, J = 8.22 Hz, 4H, H_9), 8.52 (d, J = 8.28 Hz, 4H, H_6); ^{13}C{^{1}H} NMR (DMSO-d_6, 100 MHz, 25°C): δ 10.95 (C_4), 22.75 (C_3), 49.72 (C_2), 57.92 (C_{11}), 111.83 (C_6), 112.62 (C_9), 124.53 (C_7), 124.86 (C_8), 133.35 (C_5), 133.62 (C_{10}), 178.87 (C_1). (ATR) cm^{-1}: 3025 ν(C-H)ar, 2965 ν(C-H), 1450, 1395 (δ(C=C), δ(C=N))ar, 1051, 1017 δ(C-H)ip, 755 δ(C-H)oop. HRMS-ESI (DMSO): m/z = 385.1514 ($[M-2I^-]^{2+}$), 897.2086 ($[M-I^-]^+$).

Bis(1,1'-dipropyl-3,3'-ethylenedibenzimidazolin-2,2'-diylidene)palladium(II) bromide (*C1bb*). Palladium(II) acetate (33 mg, 0.15 mmol, 1 eq), ligand **3b** (157 mg, 0.30 mmol, 2.1 eq) and sodium acetate (24 mg, 0.29 mmol, 2 eq) were dissolved in degassed DMSO (3 mL) in a round-bottom flask. The brownish mixture was stirred for 1 h at 60°C, 2 h at 80°C and 1 h at 110°C. Thus, sodium acetate (24 mg, 0.3 mmol, 2 eq) was added again and the reaction mixture was kept at 110°C for 1.5 h. After cooling to room temperature, a white suspension was obtained. Water (6 mL) was added to precipitate a grey powder. The precipitate was filtered and washed with acetone (6 mL x 6). The product was obtained as a pale grey powder. Yield: 38 mg, 27%. ^{1}H NMR (CD_3OD, 400 MHz, 25°C): δ 0.75 (t, J = 7.22 Hz, 12H, H_4), 0.87 (m, 4H, H_3), 1.75 (m, 4H, H_3), 4.23 (m, 4H, H_2), 4.42 (m, 4H, H_2), 5.50 (m, 4H, H_{11}), 5.83 (m, 4H, H_{11}), 7.45 (td, J = 0.87 Hz, J = 7.35 Hz, 4H, H_7), 7.52 (dt, J = 0.98 Hz, J = 7.52 Hz, 4H, H_8), 7.64 (d, J = 7.96 Hz, 4H, H_9), 7.90 (d, J = 8.21 Hz, 4H, H_6); ^{13}C{^{1}H} NMR (CD_3OD, 100 MHz, 25°C): δ 11.36 (C_4), 23.97 (C_3), 46.29 (C_{11}), 51.95 (C_2), 112.31 (C_6), 113.10 (C_9), 126.20 (C_8), 126.24 (C_7), 135.13 (C_5), 135.82 (C_{10}), 176.26 (C_1). (ATR) cm^{-1}: 3026 ν(C-H)ar, 2965 ν(C-H), 1451, 1395 (δ(C=C), δ(C=N))ar, 1040, 1014 δ(C-H)ip, 765 δ(C-H)oop. HRMS-ESI (CH_3OH): m/z = 399.1693 ($[M-2Br^-]^{2+}$).

■ ASSOCIATED CONTENT

Supporting Information

The Supporting Information is available free of charge on the ACS Publications website at DOI: xxx

Appendix A

CCDC XXXXXX (for **3b**), XXXXXX (for **C1a**), XXXXXX (for **C1b**) and XXXXXX (for **C1c**); contains the supplementary crystallographic data for this paper. These data can be obtained free of charge from The Cambridge Crystallographic Data Centre via www.ccdc.cam.ac.uk/data_request/cif.

■ AUTHOR INFORMATION

Corresponding Authors

*jonathan.detovar@ircelyon.univ-lyon1.fr

*Laurent.Djakovitch@ircelyon.univ-lyon1.fr

ORCID

Jonathan De Tovar: 0000-0003-1106-8003

Franck Rataboul: 0000-0002-4299-5937

Laurent Djakovitch: 0000-0001-5084-5608

Notes

The authors declare no competing financial interest.

■ ACKNOWLEDGEMENTS

Support from ANR (HYPERCAT, contract N° ANR-18-CE07-0021-03) research program ''HYPERCAT'' is gratefully acknowledged. We kindly acknowledge the 'Analytical Platform'' of IRCELYON, Centre Commun de Spectrométrie de Masse of University Lyon 1 for analyses and helpful discussions (L. Burel for TEM and N. Bonnet and P. Mascunan for ICP-OES analyses). We also thank E. Jeanneau for X-ray diffraction studies.

■ REFERENCES

(1) Kotha, S.; Lahiri, K.; Kashinath, D. *Tetrahedron* **2002**, *58*, 9633-9695.

(2) Ganesan, A. *Drug Discovery Today* **2001**, *6*, 238-241.

(3) Gómez-Villarraga, F.; De Tovar, J.; Guerrero, M.; Nolis, P.; Parella, T.; Lecante, P.; Romero, N.; Escriche, L.; Bofill, R.; Ros, J.; Sala, X.; Philippot, K.; García-Antón, J. *Dalton Trans.* **2017**, *46*, 11768-11778.

(4) Fihri, A.; Bouhrara, M.; Nekoueishahraki, B.; Basset, J.-M.; Polshettiwar, V. *Chem. Soc. Rev.* **2011**, *40*, 5181-5203.

(5) Schmidt, A. F.; Kurokhtina, A. A. *Kinetics and Catalysis* **2012**, *53*, 714-730.

(6) Djakovitch, L.; Koehler, K.; De Vries, J. G. The Role of Palladium Nanoparticles as Catalyst for Carbon – Carbon Coupling Reactions. In *Nanoparticles and Catalysis*; Astruc, D. Editor.; Wiley-VCH: Weinheim, 2008 pp 303-348.

(7) Cantillo, D.; Kappe, C. O. *ChemCatChem* **2014**, *6*, 3286-3305.

(8) Arvela, R. K.; Leadbeater, N. E.; Collins, M. J. *Tetrahedron* **2005**, *61*, 9349-9355.

(9) Morris, R. H. *Acc. Chem. Res.* **2015**, *48*, 1494-1502.

(10) Van Leeuween, P. W. N. M.; Kamer, P. C. J.; Reek, J. N. H.; Dierkes, P. *Chem. Rev.* **2000**, *100*, 2741-2770.

(11) Liang, Y.; Li, Y.; Wang, H.; Zhou, J. ; Wang, J. ; Regier, T.; Dai, H. *Nat. Mater.* **2011**, *10*, 780-786.

(12) Dudkina, Y. B.; Kohlin, K. V.; Gryaznova, T. V.; Islamov, D. R.; Kataeva, O. N.; Rizvanov, I. Kh.; Levitskaya, A. I.; Fominykh, O. D.; Balakina, M. Y.; Sinyashin, O. G.; Budnikova, Y. H. *Dalton Trans.* **2017**, *46*, 165-177.

(13) Matheu, R.; Garrido-Barros, P.; Gil-Sepulcre, M.; Ertem, M. Z.; Sala, X.; Gimbert-Suriñach, C.; Llobet, A. *Nat. Chem. Rev.* **2019**, *3*, 331-341.

(14) Frey, G. D.; Lavallo, V.; Donnadieu, B.; Schoeller, W. W.; Bertrand, G. *Science* **2007**, *316*, 439-441.

(15) Wang, Y.; Xie, Y.; Wei, P.; King, R. B. Schaefer III, H. F.; Schleyer, P. V. R.; Robinson, G. *Science* **2008**, *321*, 1069-1071.

(16) Lee, H. M.; Lu, C. Y.; Chen, C. Y., Chen, C. W.; Lin, H. C.; Chiu, P. L.; Cheng, P. Y. *Tetrahedron* **2004**, *60*, 5807-5825.

(17) Scherg, T.; Schneider, S. K.; Frey, G. D.; Schwarz, J.; Herdtweck, E.; Herrmann, W. A. *Synlett* **2006**, *18*, 2894-2907.

(18) Baker, M. V.; Skelton, B. W.; White, A. H.; Williams, C. C. *J. Chem. Soc. Dalton Trans.* **2001**, *2*, 111-120.

(19) Baker, M. V. ; Brown, D. H.; Simpson, P. V.; Skelton, B. W.; White, A. H.; Williams, C. C. *J. Organomet. Chem.* **2006**, *691*, 5848-5855.

(20) Baker, M. V.; Brown, D/ H/; Simpson, P. V.; Skelton, B/ W/; White, A. H. *Dalton Trans*. **2009**, *35*, 7294-7307.

(21) Jothibasu, R.; Huynh, H. V. *J. Organomet. Chem*. **2011**, *696*, 3369-3375.

(22) Herrmann, W. A.; Reisinger, C.-P.; Spielger, M. *J. Organomet. Chem.* **1998**, *557*, 93-96.

(23) Zhang, C.; Trudell, M. L. *Tetrahedron Lett*. **2000**, *41*, 595-598.

(24) Ahrens, S.; Zeller, A.; Taige, M.; Strassner, T. *Organometallics* **2006**, *25*, 5409-5415.

(25) Steffen, W. L.; Palenik, G. J. *Inorg. Chem.* **1976**, *15*, 2432-2439.

(26) Berding, J.; Lutz, M.; Spek, A. L.; Bouwman, E. *Organometallics* **2009**, *28*, 1845-1854.

(27) Hahn, F. E.; von Fehren, T.; Lügger, T. *Inorg. Chim. Acta* **2005**, *358*, 4137-4144.

(28) Brookhart, M.; Green, M. L. H.; Parkin, G. *PNAS*, **2007**, *104*, 6908-6914.

(29) Livingstone, S. E. *J. Proc. R. Soc. N. S. Wales* **1952**, *86*, 32-37.

(30) Newkome, G. R.; Gupta, V. K.; Taylor, H. C. R.; Fronczek, F. R. *Organometallics* **1984**, *3*, 1549-1554.

(31) Beller, M.; Fischer, H.; Herrmann, W. A.; Öfele, K.; Broβmer, C. *Angew. Chem. Int. Ed. Engl.* **1995**, *34*, 1848-1849.

(32) Blanksby, S. J.; Ellison, G. B. *Acc. Chem. Res.* **2003**, *36*, 255-263.

(33) Astakhov, A. V.; Khazipov, O. V.; Chernenko, A. Y.; Pasyukov, D. V.; Kashin, A. S.; Gordeev, E. G.; Khrustalev, V. N.; Chernyshev, V. M.; Ananikov, V. P. *Organometallics* **2017**, *36*, 1981-1992.

(34) Favier, I.; Lavedan, P.; Massou, S.; Teuma, E.; Philippot, K.; Chaudret, B.; Gómez, M. *Top. Catal.* **2013**, *56*, 1253-1261.

(35) Hayes, J. M.; Viciano, M.; Peris, E.; Ujaque, G.; Lledós, A. *Organometallics* **2007**, *26*, 6170-6183.

(36) Nemcsok, D.; Wichmann, K.; Frenking, G. *Organometallics* **2004**, *23*, 3640-3646.

(37) Khramov, D. M.; Lynch, V. M.; Bielawski, C. W. *Organometallics* **2007**, *26*, 6042-6049.

(38) Tolman, C. A. *Chem. Rev.* **1977**, *77*, 313-348.

(39) Rossi, L. M.; Fioro, J. L.; Garcia, M. A. S.; Ferraz, C. P. *Dalton Trans.* **2018**, *47*, 5889-5915.

(40) Louie, J.; Hartwig, J. F. *Angew. Chem. Int. Ed. Engl.* **1996**, *35*, 2359-2361.

(41) Whitesides, G. M.; Hackett, M.; Brainard, R. L.; Lavalleye, J. P. P. M.; Sowinski, A. F.; Izumi, A. N.; Moore, S. S.; Brown, D. W.; Staud, E. M. *Organometallics* **1985**, *4*, 1819-1830.

(42) Oliveira, R. L.; He, W.; Klein Gebbink, R. J. M.; de Jong, K. P. *Catal. Sci. Technol.* **2015**, *5*, 1919-1928.

(43) Górna, M.; Szulmanowicz, M. S.; Gniewek, A.; Tylus, W.; Trzeciak, A. M. *J. Organomet. Chem.* **2015**, *785*, 92-99.

(44) Eremin, D. E.; Denisova, E. A.; Kostyukovich, A. Y.; Martens, J.; Berden, G.; Oomens, J.; Khrustalev, V. N.; Chernyshev, V. M.; Ananikov, V. P. *Chem. Eur. J.* **2019**, *25*, 16564-16572.

(45) CrysAlisPro Software System, version 1.171.40.53. Rigaku Oxford Diffraction, **2019**.

(46) Sheldrick, G. M. *Acta Cryst.* **2015**, *71*, 3-8.

(47) Dolomanov, O. V.; Bourhis, L. J.; Gildea, R. J.; Howard, J. A. K.; Puschmann, H. *J. Appl. Cryst.* **2009**, *42*, 339-341.

(48) Lin, Y.-R.; Chiu, C.-C.; Chiu; H.-T.; Lee, D.-S.; Lu, T.-J. *Appl. Organometal. Chem.* **2018**, *32*.

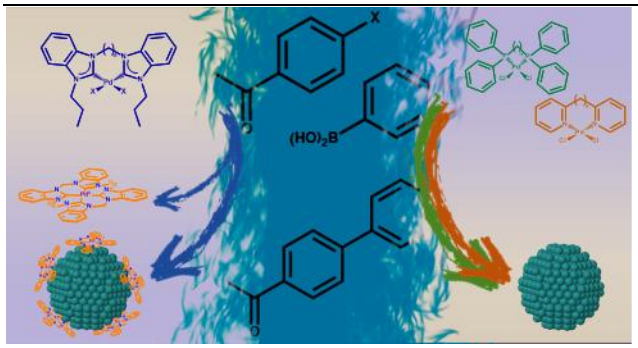
X
O
$(HO)_2B$
O